Calorimetric determination of wet snow liquid water content

D Fasani*[1,2], F M Cernuschi[2], L P M Colombo[1]

[1]Politecnico di Milano, via Raffaele Lambruschini 4, 20156 Milano, Italy

[2]RSE S.p.A., via Rubattino 54, 20134 Milano, Italy

*Corresponding author: damiano.fasani@polimi.it

ABSTRACT.

Liquid water content (lwc) of wet snow is a fundamental parameter in determining snow properties like its strength and adhesion force to surfaces. Among the different methods available for the measurement of the lwc, this paper focuses on melting calorimetry: known masses of hot water and snow are mixed into a thermally insulated container, and the lwc is obtained from the difference between the initial hot water temperature and the final mixing temperature. Tests with "synthetic" wet snow samples whose liquid content is known in advance are carried out to assess the method, showing that the method overestimates the liquid content by a variable amount that seems to depend on the test parameters. In order to account for the heat capacity of the calorimeter, which is not negligible, a constant in terms of equivalent hot water mass (E) is introduced. However, its value also depends on the test conditions. Hence, a correlation between E and the test parameters is found, and the measurements were repeated using a container of a different material, showing a similar behavior. Eventually, a discussion about the effects of choosing different hot water masses and hot water-to-snow mass ratios on measurement accuracy is provided.

KEYWORDS: Wet snow, calorimetry

INTRODUCTION: WET SNOW ACCRETION AND LIQUID CONTENT MEASUREMENT

Snow accumulation on overhead powerlines during wet snow events is regarded as a severe threat to the grid: it is reported that the overload of snow on power lines is the principal cause of major power outages during the winter season in Italy (Marcacci, Lacavalla, & Pirovano, 2019). The presence of liquid water in the snowflakes makes them sticky and promotes the adhesion to solid bodies exposed to the airflow. Moreover,

it determines faster inter-grain bonding, resulting in an increased strength of the snow (Brun, 1989). This leads to the formation and growth of thick wet-snow sleeves on the conductors, which can eventually lead to the breaking of the conductor itself and even to the infrastructure collapse. Liquid water content (lwc) of wet snow, defined as the liquid fraction (either by mass or volume) of snow, is a fundamental parameter in determining it properties like its mechanical strength and adhesion strength to surfaces (Hefny, Kollar, Farzaneh, & Payrard, 2009), making its measurement of crucial importance. Over the years, different methods have been developed for this purpose: calorimetric methods (e.g.: melting and freezing calorimetry), dilution methods, and dielectric methods. Melting calorimetry (Kawashima, Endo, & Takeuchi, 1998) is an easy and inexpensive method, other than quick to implement, as the melting of the solid fraction of snow in hot water takes few seconds; however, it is not comparable to other calorimetric methods in terms of sensitivity. Freezing calorimetry (Jones, Rango, & Howell, 1983) is performed by mixing wet snow and a freezing agent, usually silicone oil, in a thermally insulated container and by measuring the temperature rise of the freezing agent, as the heat gained by the fluid is the one lost by water freezing and sample subcooling. The dilution method (Davis, Dozier, LaChappelle, & Perla, 1985) is performed by saturating a wet snow sample with an aqueous solution containing a low concentration of a certain impurity, extracting the liquid from the sample (e.g.: by centrifugation) and measuring how much the original solution has been diluted by the water present in the snow sample. The concentration variation can be measured in different ways according to the kind of solution: for example, using a low concentration HCl solution and measuring the change in electrical conductivity related to the ion concentration. This method requires a careful control of the temperature, as small deviations from zero can determine melting/freezing. Dielectric methods are based on the idea that the permittivity of snow depends on its density and volumetric liquid water content (meaning that they need a separate measurement for density). The Snow Fork (Sihvola & Tiuri, 1986) and the Denoth meter (Denoth, 1994) are both examples of dielectric methods: however, they require a considerable amount of snow as they were developed for snowpack measurement. This paper focuses on melting calorimetry aiming at putting in evidence how the test conditions affect both the measurement uncertainty and the sensitivity.

MATERIALS AND METHODS: MELTING CALORIMETRY

The measurement is performed by mixing known masses of hot water (m_w) and wet snow (m_{sn}) into a thermally insulated container: the final temperature of the mix depends on the initial lwc of snow, as the heat lost by hot water – initially at temperature T_1 – is equal to the one needed to melt the solid fraction of the snow sample and bring the whole sample at the final temperature T_2. The test is carried out as follows: 1) The mass of the empty container (M_T) is measured; 2) A certain amount of water between 33 and 35°C is poured into the container and gently shaken; the total mass (M_1) and the water temperature (T_1) are measured; 3) the snow sample is put into the container and the final mass (M_2) and temperature of the mix (T_2) are measured. Considering that $m_w = M_1 - M_T$ and $m_{sn} = M_2 - M_1$, the measured lwc is:

$$lwc = 1 - k[R(T_1 - T_2) - T_2] \quad (1)$$

$$R = (M_1 - M_T)/(M_2 - M_1),\ k = c_{p,w}/L_f = 1.25 \cdot 10^{-2}\ \mathrm{K}^{-1} \quad (2)$$

where $c_{p,w}$ is water specific heat capacity at constant pressure and L_f is ice melting latent heat, while R is defined as the hot water-to-snow mass ratio.

Two containers have been used in this work: the container initially chosen is a commercial 1 L thermal insulating stainless steel (AISI 304) bottle with a 50 mm opening; a hole has been drilled in its lid enabling the insertion of a temperature probe inside it; the second container is a 1L Dewar with a 75 mm opening and a Styrofoam lid with a hole in it. The temperature measurement equipment consists of a Pt100 RTD probe, the signal of which is read by a HD2107.1 logger, both by Delta OHM. The overall measurement uncertainty $u_{T_{RTD}}$ is 0.05°C. The masses are measured on a Sartorius FB2CCE-S scale, with a measurement uncertainty u_M=0.01 g. To assess the validity and accuracy of the method, tests with "synthetic" snow samples were performed: dry snow at $T_s = -3/-2$ °C and water at $T_m = 0$ °C were used to prepare equivalent wet snow samples in the range $lwc_s = 0 - 30$ % by mass; the two phases were put in the calorimeter separately, measuring each time the total mass, so that the liquid content of these surrogate samples is known a priori. The subcooling ($\Delta T_{sub} = T_s - T_m$) of the dry snow is required to make sure that its original water content is zero; this also means that the real liquid content (lwc_r) of such equivalent samples need to be corrected to account for the

ice sensible heat according to equation (3). Dry snow temperature is measured with two HI9851 thermometers by Hanna Instruments ($u_{T_s} = 0.2$°C)

$$lwc_r = lwc_s - (1 - lwc_s)\frac{c_{p,I}}{L_f}\Delta T_{sub} \qquad \text{with} \qquad lwc_s = \frac{M_2 - M_{2d}}{M_2 - M_1} \tag{3}$$

where $c_{p,I}$ and M_{2d} are the ice specific heat and the total mass of the container after only ice has been introduced, respectively. Preliminary tests have shown that the method always overestimates the actual lwc of the snow by a variable amount (between 4 and 10% in absolute value) that seems to depend on the test parameters, such as snow and hot water masses and their ratio, and the lwc itself, meaning that the heat capacity of the container is not negligible. To account for it, an additional term E (hereafter named *calorimeter constant*) representing an equivalent hot water mass was introduced, as shown in equation (4):

$$lwc = 1 - k\left[\frac{(M_1 + E) - M_T}{M_2 - M_1}(T_1 - T_2) - T_2\right] \tag{4}$$

Hence, assuming $lwc = lwc_r$, the calorimeter constant is obtained as:

$$E = \frac{M_2 - M_1}{T_1 - T_2}\left[\frac{1 - lwc_r}{k} + T_2\right] - (M_1 - M_T) \tag{5}$$

However, the same tests seem to indicate that the calorimeter constant is in fact not constant, but it may depend on the test parameters themselves and the lwc of the synthetic samples: as discussed in the following sections, this suggests that thermal equilibrium inside the container may not be achieved, and that the results may depend on the experimental procedure as well, particularly on how and how long the container is shaken to achieve the mixing of hot water and snow.

Test conditions and procedure

To identify the relation between the test parameters and the quantity E, an extensive experimental campaign using the aforementioned equivalent samples was carried out in the cold laboratories of the WSL Institute for Snow and Avalanche Research SLF in Davos, Switzerland: the free parameters chosen are the lwc of the sample, the hot water mass m_w and the hot water to snow sample mass ratio R. The range of variation of these parameters (Table 1) was chosen according to practical requirements: the snow mass is limited to the

typical size of the samples used for mechanical tests, while the ratio R (and m_w consequently) is limited by measurement uncertainty requirements since the lwc uncertainty increases with R. This will be discussed in a dedicated section.

lwc_s [% m]	m_w [g]	R [-]	T_1 [°C]
0, 10, 20, 30	260, 500	4, 6, 9, 13	33 ÷ 35

Table 1. Test conditions.

The method adopted for the two different containers differs owing to their characteristics:

- The steel container is vigorously shaken after the snow sample is introduced; the temperature is measured and then the container is shaken again: if the temperature has increased compared to the previous measurement, the procedure is repeated until no further change in temperature is observed (with a tolerance of 0.01 °C).
- The Dewar glass wall makes the attempt to reach a condition close to equilibrium impractical, since its comparatively lower thermal diffusivity increases the time required to achieve such condition; instead, a gentler mixing of the two masses by circular horizontal motion was preferred: this was made to avoid the slow rising in the final temperature over time – a phenomenon observed when no shaking at all took place – as a consequence of heat exchange from the walls to the water. This approach is sensitive to the duration of the mixing, so it was set to a duration of 20 s for every test.

For the steel container, a second experimental campaign was carried out in RSE Artificial Snow Lab (Piacenza, Italy) to verify the validity of the empirical relation obtained from the first campaign between E and the test parameters. Following the same procedure described above, a limited number of samples spanning the whole range of R, m_w and lwc was chosen. A comparison between the predicted value of E and the value retrieved from experimental data is then provided. The steel container was then dismantled, and the mass of internal wall m_{st} was measured: its equivalent in term of water mass E_{st} is computed as in equation (6), where $c_{p,st} = 477\ \mathrm{J/kg\ K}$ is the specific heat capacity of AISI 304 stainless steel at $T = 300\ \mathrm{K}$ (Incropera & DeWitt, 1996). This value is then compared to the corrective term E obtained from experimental data.

$$E_{st} = \frac{c_{p,st}}{c_{p,w}} m_{st} \tag{6}$$

General considerations on liquid water content uncertainty

The well-known propagation error approach was used to evaluate the uncertainty of lwc:

$$u_{lwc} = \sqrt{\sum_i \left(\frac{\partial lwc}{\partial x_i} u_{x_i}\right)^2} \tag{7}$$

where $x_i = T_1$, T_2, M_T, M_1, M_2, and E. For temperature and mass, the respective instrumental uncertainties were used. A discussion on the melting calorimetric method uncertainty can be already found in Kawashima *et al.* [4], where it is shown that the lwc uncertainty decreases as the ratio R decreases: in fact, as reported in Figure 1, the sensitivity of the method to the presence of water – represented here by the difference ΔT_2 between the actual final temperature T_2 and the value it would assume if the snow was dry ($T_{2,dry}$) – increases as the ratio R decreases and, consequently, the overall uncertainty decreases.

The existence of a calorimeter constant introduces an additional uncertainty contribution; as shown in Figure 2, while the effect of the value of the constant E itself is very mild, the overall uncertainty increases significantly with u_E, especially for smaller values of water mass m_w (black lines): this can be easily understood by considering that the contribution of the calorimeter constant uncertainty to the overall uncertainty can be written as:

$$\left|\frac{\partial lwc}{\partial E}\right| u_E = |1 + kT_1 - lwc| \frac{u_E}{m_w\left(1 + \frac{1}{R}\right) + E} \tag{8}$$

A new quantity is defined:

$$r_{u_E} = \frac{u_E}{m_w\left(1 + \frac{1}{R}\right) + E} = \frac{u_E}{m_{HE,tot}} \tag{9}$$

where the denominator represents the total mass involved in the heat exchange. Figure 3 represents the overall lwc uncertainty as a function of R for two values of r_{u_E} and different values of E and m_w; it is evident that the curves with the same r_{u_E} are mostly coincident, regardless of the values of E and m_w. Therefore, it can be concluded that when the calorimeter constant cannot be determined with a sufficiently small uncertainty, greater masses of snow/water are suggested (compatibly with the constrains on R)

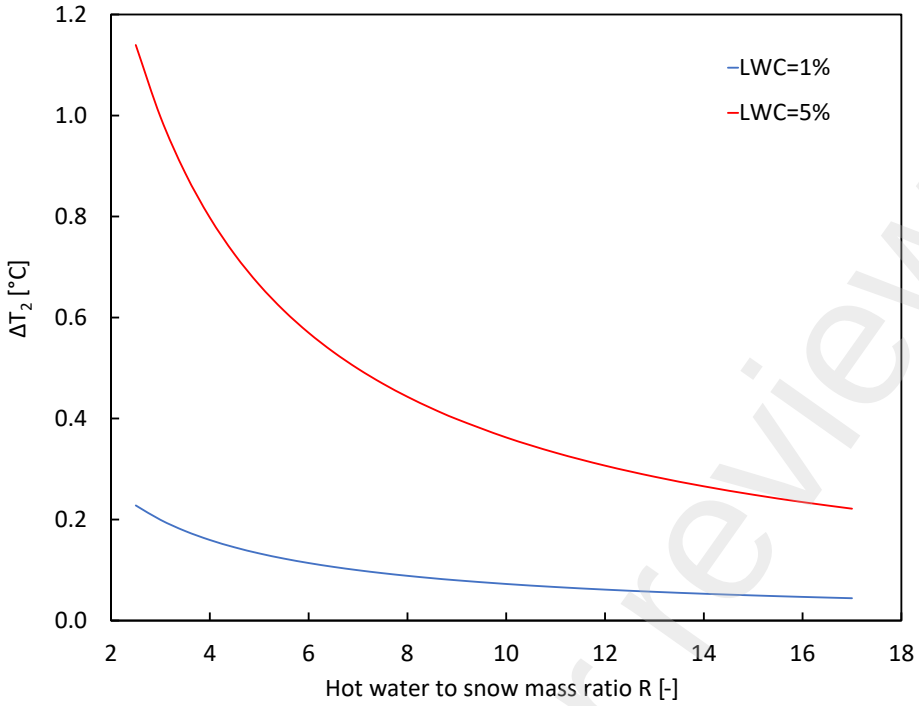

141

142 **Figure 1.** Sensitivity of the final temperature to the presence of liquid with respect to dry snow case ($\Delta T_2 = T_2$

143 $- T_{2,dry}$) as a function of the hot water to snow mass ratio R.

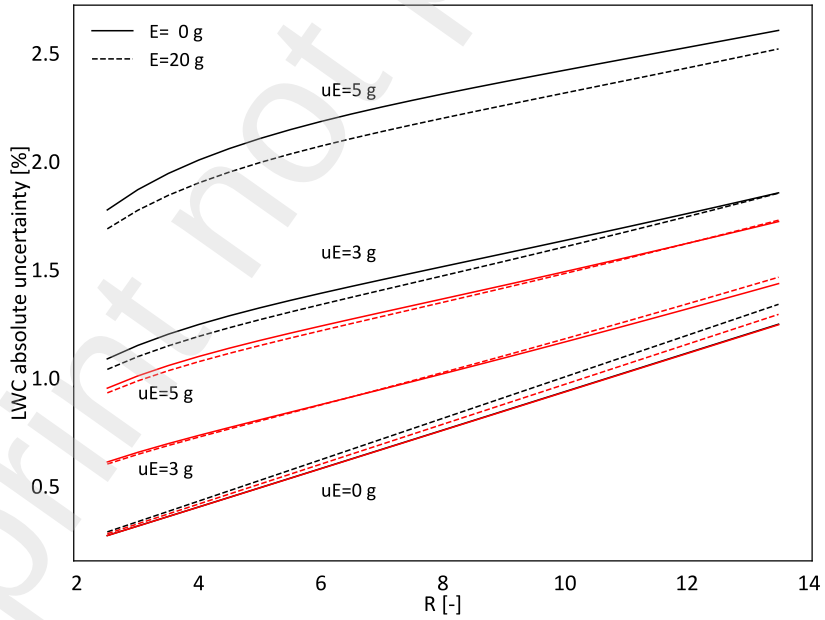

144

145 **Figure 2.** Liquid water content absolute uncertainty dependence on R, E and u_E for $T_1 = 34$ °C, $m_w = 260$ g

146 (black lines) and 500 g (red lines), $lwc = 15$ %

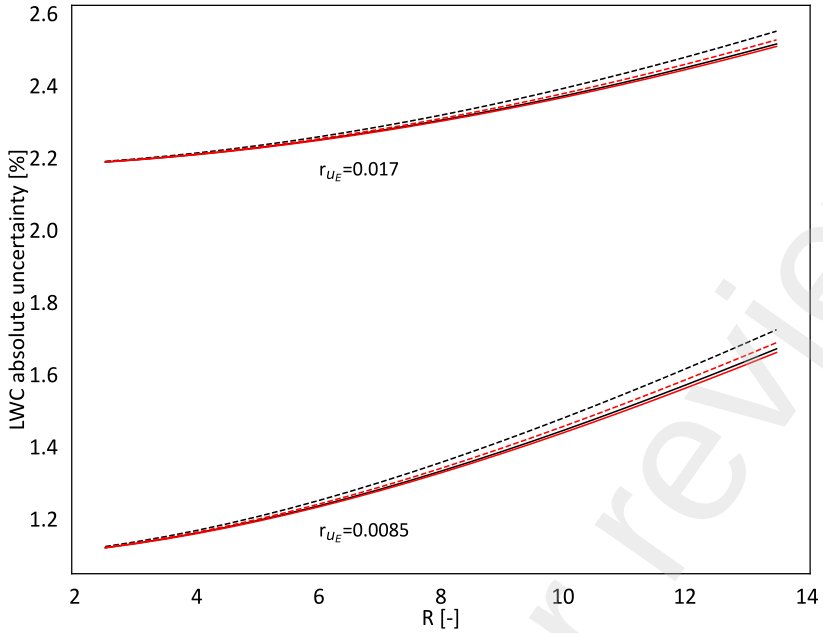

147

148 **Figure 3.** Liquid water content absolute uncertainty dependence on R, E and the parameter r_{u_E} for $T_1 = 34\ °C$,

149 $m_w = 260\ g$ (black lines) and $500\ g$ (red lines), $lwc = 15\ \%$ as a function of the hot water to snow mass ratio

150 R

151

152 ## RESULTS AND DISCUSSION

153 ### Steel calorimeter

154 The results of the SLF experimental campaign are reported in Figure 4, which represents the constant of the

155 steel calorimeter computed as in equation (5) as a function of the measured liquid water content and for

156 different values of hot water mass and hot water to snow mass ratios. It is shown that the constant decreases

157 as the lwc and the ratio R increase; however, given a certain value of R, it seems to be independent of the

158 hot water mass, as data points tend to align in a single series, regardless of the actual hot water and snow

159 masses; this has been confirmed by performing a Tukey test at 95% confidence level (Figure 5), showing that

160 the average calorimeter constant of data series with different R is significantly different, while for data series

161 with the same ratio R it is not.

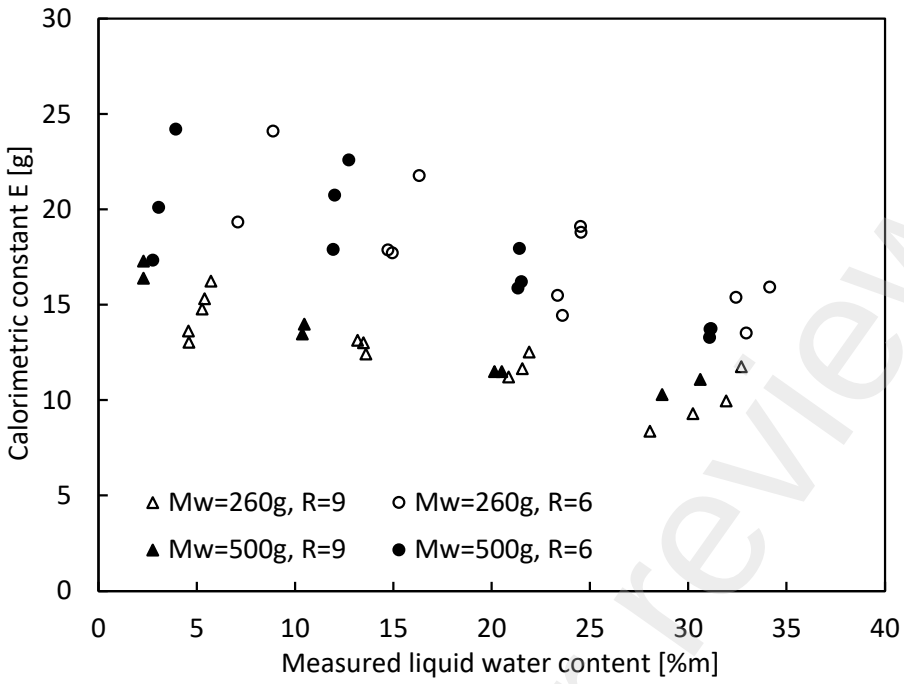

Figure 4. Calorimeter constant vs measured liquid water content for the steel container.

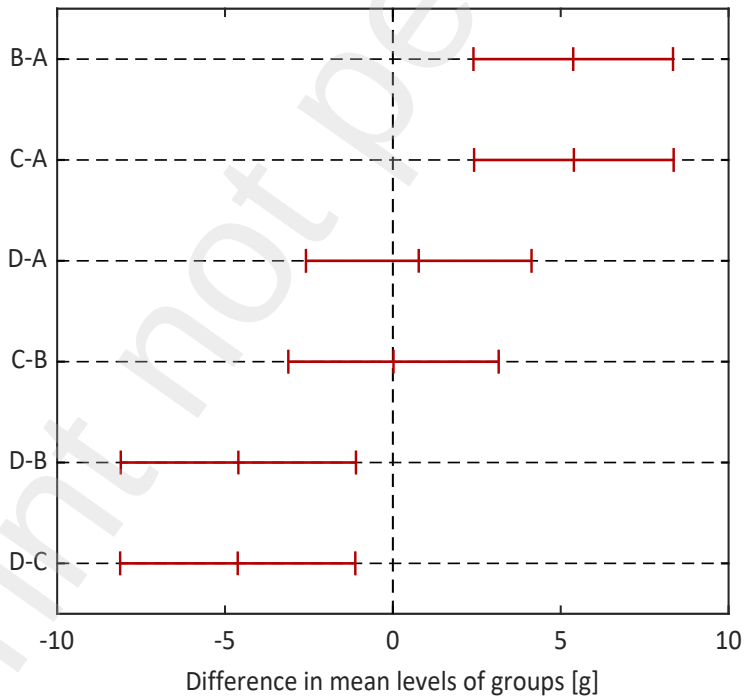

Figure 5. Results of a Tukey test at 95% confidence level of the mean values of the data series for the calorimeter constant of the steel container: each horizontal segment represents the 95% confidence interval for the difference between the mean values (mid ticks) of the corresponding pair of data series reported on the vertical axis.

Group	A	B	C	D
$R\ [-]$	9	6	6	9
$m_w\ [g]$	260	260	500	500

Table 2. Test parameters for each data series of the steel container

Collected data seem to suggest that the constant E increases with the amount of heat exchanged relative to the hot water mass: indeed, for a given hot water mass, the bigger the snow sample at fixed lwc, the larger the heat exchanged; moreover, at given hot water and snow masses, the lower the LWC, the larger the heat required to melt the solid fraction of the sample. Therefore, denoting snow mass water equivalent the snow sample mass if its ice fraction was converted to a corresponding water mass $m_{w,eq}$ that exchanges the same amount of heat with the hot water and the calorimeter according to equation (10),

$$m_{sn}[(1 - lwc_r)L_f + c_{p,w}T_2] = m_{w,eq}c_{p,w}T_2 \tag{10}$$

a new parameter r_{eq} is introduced as:

$$r_{eq} = \frac{m_{w,eq}}{m_w + E} = \frac{1 - lwc_r + kT_2}{kT_2(1 + E/m_w)R} \tag{11}$$

By substitution of equation (4) in the previous expression, it can be shown that the mass ratio can be reduced to the temperature difference ratio reported below,

$$r_{eq} = \frac{T_1 - T_2}{T_2 - T_0} \tag{12}$$

where $T_0 = 0°\mathrm{C}$ is the melting temperature. Figure 6 reports the obtained values of E (black markers) represented as a function of the equivalent ratio, where it is possible to identify a linear trend irrespective of lwc, R or m_w. The solid black line represents the linear regression of the data, while the dashed lines represent the upper and lower bounds obtained when considering its predicted uncertainty, computed with the propagation formula as shown in more detail in the Appendix. The result of such analysis is reported in equation (13).

$$E = 29.3\ r_{eq}\,,\ u_E = \sqrt{11.2\ r_{eq}^2 + 3.5} \tag{13}$$

These equations are used to adjust the value of the measured lwc and to obtain a prediction of its uncertainty, whose maximum value was found to be 1.5 % absolute.

Additionally, the chart also reports the results of the second experimental campaign (red markers), showing good agreement with previous data and with the empitical corrective relation, suggesting that equation (13) is representative of the behavior of the corrective term as a function of the equivalent ratio r_{eq} within its experimental uncertainty.

The measured mass of the internal vessel of the steel calorimeter m_{st} is 159.4 g, corresponding to an equivalent water mass E_{st} of 18.2 g, which has the same order of magnitude of the values obtained experimentally; however, about 27 % of the latter – which drops below 9 % if the uncertainty is accounted for – exceeds the value of E_{st}; this discrepancy could be attributed to the fact that other parts of the bottle contribute to the calorimeter heat capacity, such as the additional threaded metal around the opening (which was destroyed in the process of extracting the internal vessel and therefore could not be measured), where the internal and external walls meet.

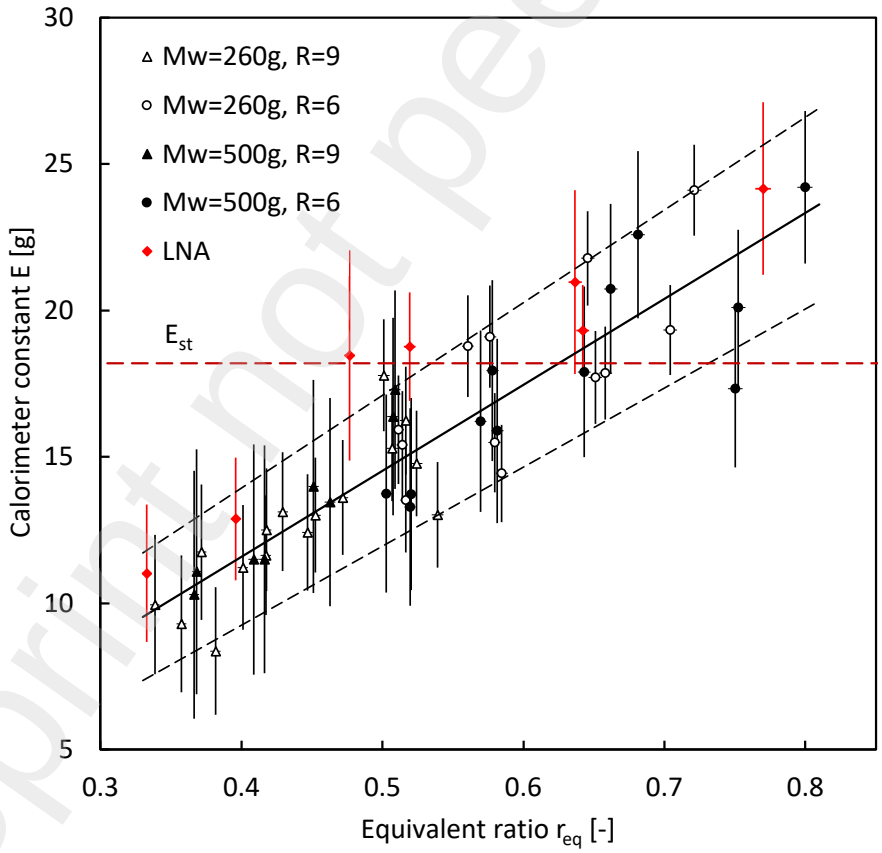

Figure 6. Calorimeter constant as a function of the ratio r_{eq}. Black points: data from the experimental campaign at SLF, Switzerland. Red points: data from the experimental campaign in RSE Artificial Snow Lab (LNA). Solid line: data linear regression based on the SLF campaign. Upper and lower dashed lines: obtained

by adding and subtracting respectively the predicted uncertainty from the predicted value of the calorimeter constant.

Figure 7 shows the absolute lwc uncertainty predicted by making use of the relations (13) for the range of operating conditions considered in this work as a function of R: contrary to what stated in the previous section – where it was shown that u_{lwc} is monotonically increasing with R – for certain operating conditions, especially for $m_w = 260$ g, the uncertainty shows a minimum for moderate values of R and an increase at the extremes of the range: this is due to the increase of the uncertainty of the calorimeter constant at lower values of R, as predicted by equation (13). The influence of u_E decreases for bigger water masses ($m_w = 500$ g), as already highlighted in Figure 2, leading to an overall decrease in the combined uncertainty and a mor pronounced dependence on the ratio R.

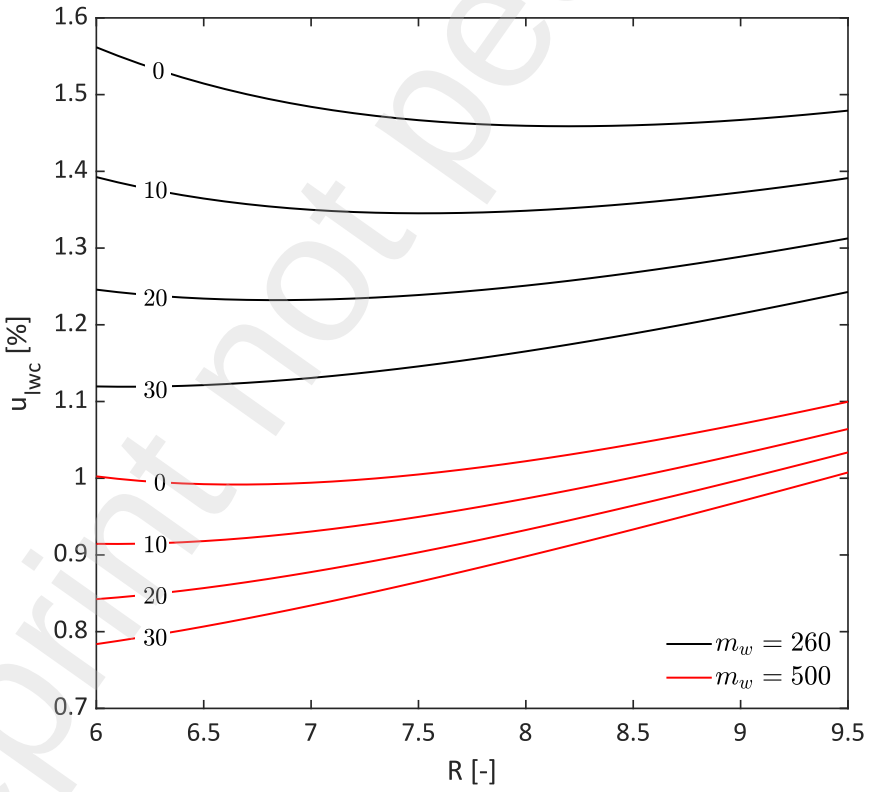

Figure 7. Liquid water content uncertainty as a function of R as predicted by equation (13). The numbers on the curves represent the liquid water content.

Finally, Figure 8 compares the real lwc (computed as in equation (3)) and the measured lwc adjusted using equation (13), where it is confirmed that the latter agrees with the former with a maximum deviation comparable to the resulting measurement uncertainty (less than ± 1.5 %, dashed lines).

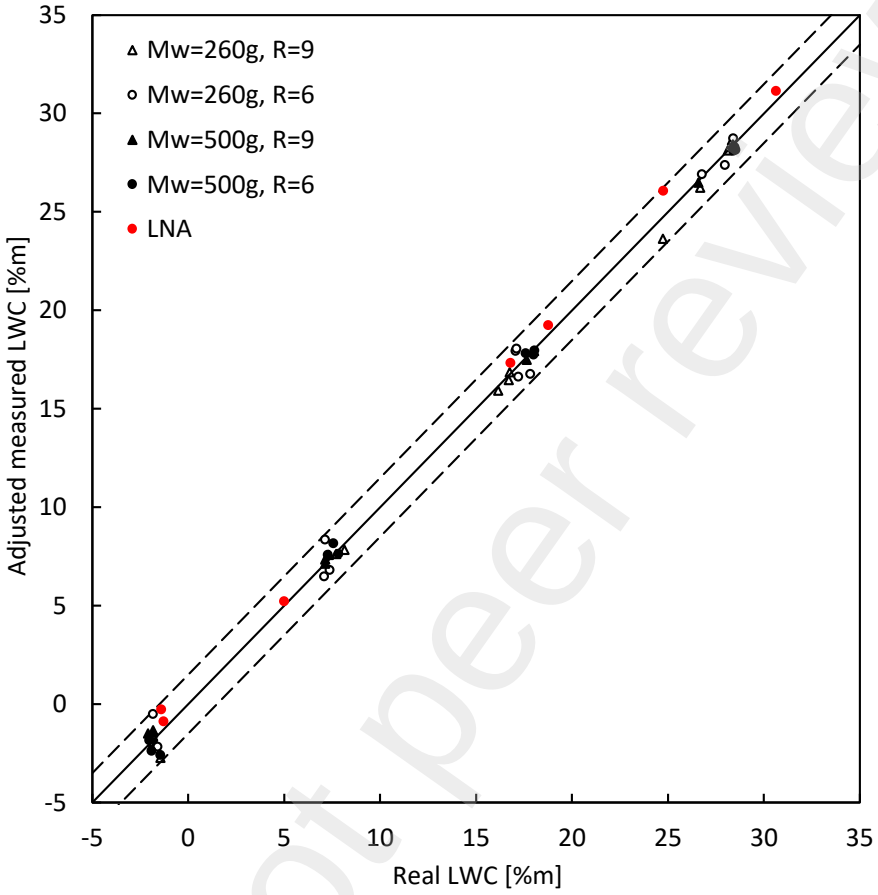

Figure 8. Adjusted lwc vs real lwc for steel calorimeter. Dashed lines represent the max uncertainty ± 1.5 %. Negative values are the result of subcooling of the snow used to prepare the samples, which leads to an apparently negative lwc when no water is added.

It is worth pointing out a behavior observed during the experimental campaign and that cannot be retrieved from the data presented here: higher values of r_{eq} – which is the consequence of lower R and/or lower lwc – lead to longer total mixing time before the final temperature T_2 stabilizes. This is even more evident outside the range of R considered here, where it was not possible to obtain valid measurements with the methodology presented; in particular:

- for $R < 6$, the raise of the final temperature is very slow during the mixing, to the point that a stable value of T_2 could not be reached;

- for $R > 9$, the final temperature shows the opposite behavior since it constantly decreases as the mixing process goes on.

Considering that the higher R, the higher T_2 (since T_1 is kept in a narrow range) and that the ambient temperature is almost constant, it is likely that heat losses during the mixing, mainly through the lid, are larger when T_2 is higher, i.e., when R is higher. Therefore, a possible explanation involves a balance between the heat lost to the environment and the heat transfer from the internal walls to the water during the mixing: for high value of R the first prevails and T_2 decreases; for lower R the latter prevails and T_2 increases. Further investigation would be required to verify this hypothesis, for example, by studying the effect of different initial temperature and ambient temperature.

Dewar

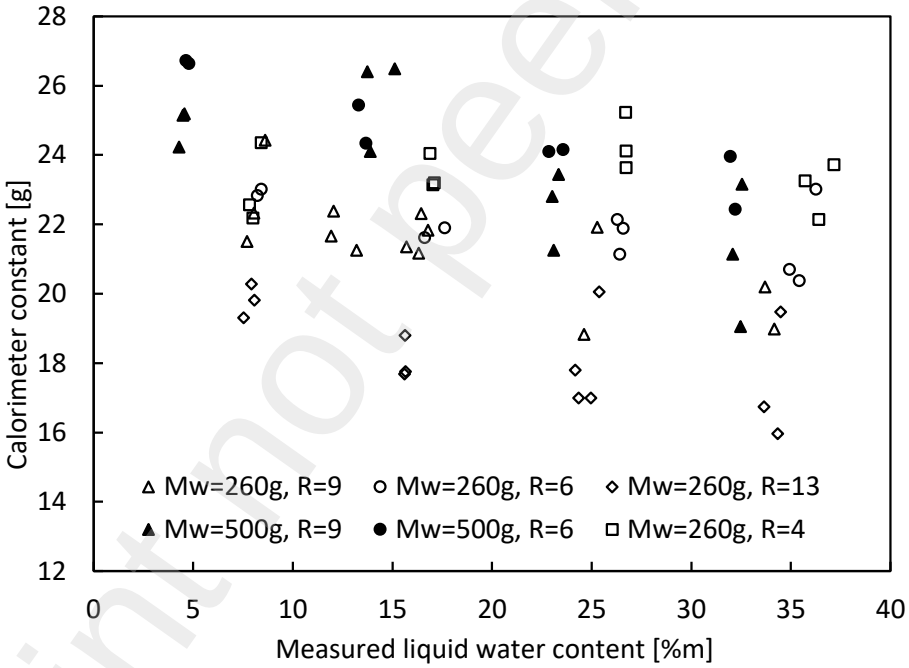

Figure 9. Calorimeter constant vs. measured liquid water content for the Dewar.

Figure 9 shows the calorimeter constant as a function of lwc. Compared to the case of the steel container, the dependence on lwc is much less pronounced. Moreover, the data points are more scattered, and the different series cannot be clearly separated on the basis of the hot water mass and the ratio R, with the

notable exception of Group C (see Table 3). The interpretation of the results of the Tukey test reported in Figure 10 is also less intuitive: however, the following observations can be made:

- The average of Group C ($R = 13$,$m_w = 260\ g$) is significantly different from any other group
- Groups with the same R but different water masses (A-D, B-E) seems to have statistically different averages
- Groups with the same water mass but different R (A-B, D-E) seems not to have statistically different averages (with the exception of Group C, $R = 13$)

The interpretation of these result is not as straightforward as in the previous case, and it will be the object of further analysis.

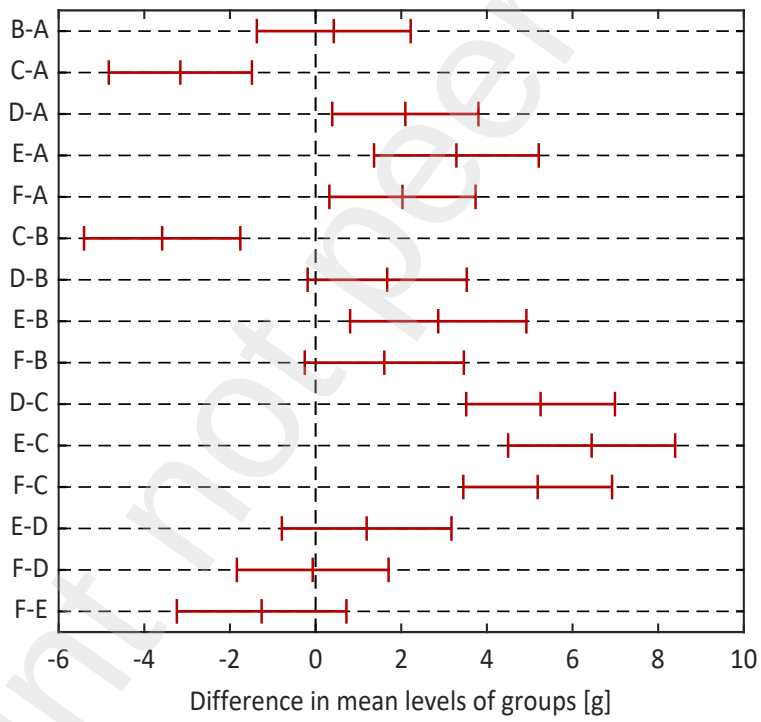

Figure 10. Results of a Tukey test at 95% confidence level of the mean values of the data series for the calorimeter constant of the Dewar.

From a practical perspective, it is suggested to use the average calorimeter constant of all data series and standard deviation as its uncertainty for every value of lwc: Figure 11 shows the comparison between real and measured lwc adjusted to account for the calorimeter constant, leading to a maximum absolute

265 deviation of 2.5 %, while its maximum uncertainty value is 2 %, which is reached, as expected, for a value of

266 $R = 13$, while the uncertainty for $R = 4$ is less than 1 %.

267

Data series		A	B	C	D	E	F	All
M_w	$[g]$	260	260	260	500	500	260	-
R	$[-]$	9	6	13	9	6	4	-
E	$[g]$	21.4	21.9	18.3	23.5	24.7	23.5	22.0
σ_E	$[g]$	1.4	0.9	1.4	2.2	1.5	0.9	2.5

268 **Table 3.** Test parameters for each data series of the Dewar with respective average calorimeter constants

269 and standard deviations

270

271 It is worth noting however, that, while in the case of the steel bottle the parameter R was limited within a

272 narrow range due to the limited validity of the correlation giving the corrective term, this combination of

273 method and container allows for a wider range of the parameter. On one hand, it is possible to make

274 measurements with the most desirable lower ratios, on the other such a configuration is more versatile when

275 the ratio R cannot be set in advance, if higher uncertainty it is acceptable.

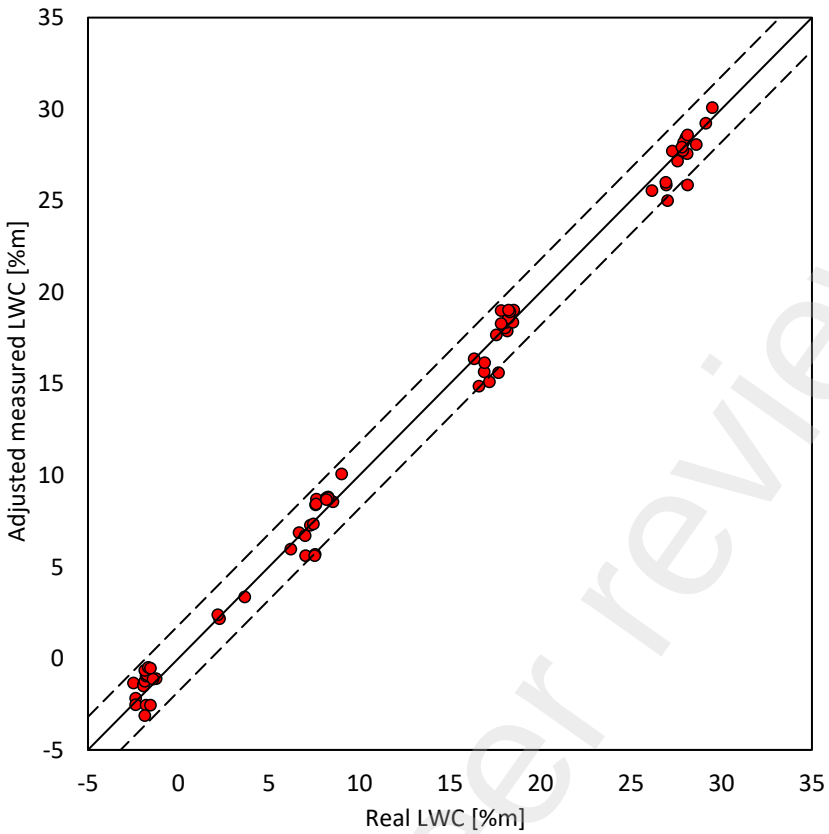

Figure 11. Adjusted LWC vs real LWC for the Dewar. Dashed lined represent the max uncertainty ± 2 %

CONCLUSIONS

The value of the calorimeter constant and its dependence on the test parameters is considerably influenced by the test procedure, especially the mixing step after the snow sample is inserted into the container, rather than the nature of the container itself. The measurement with the steel container shows a clear trend in the calorimeter constant, although limited to a narrow range of hot water-to-snow mass ratios; particularly, it will be necessary to adjust the method adopted here to make it more suitable for those values of R that can guarantee the lowest possible uncertainty. Moreover, tests should be performed to verify the effect of the ambient temperature – and thus the heat loss – on the value of the constant.

On the other hand, the Dewar and the relative procedure seems to be suited to a wider range of R; however, given the lack of a clear trend with respect to the test parameters, and the subsequent adoption of an averaged calorimeter constant, the uncertainty is more significantly affected at higher values of the hot water-to-snow mass ratios; therefore, further investigation is required to understand the effect of the test

parameters, as recognizing a trend in the data could avoid the need to rely on an average constant, leading to a decrease in the measurement uncertainty.

AKNOWLEDGEMENT

The authors would like to thank Martin Shneebeli, Henning Loewe, Matthias Jaggi and everyone else from the Physics of Snow research group at SLF in Davos, Switzerland, and Giorgio Santucci De Magistris and the Materials for Energy research group at RSE in Piacenza, Italy, for their support during the experimental activity.

REFERENCES

Brun, E. (1989). Investigation on wet snow metamorphism in respect of liquid water content. *Annals of Glaciology, 13*, 22-26. doi:10.3189/s0260305500007576

Davis, R. E., Dozier, J., LaChappelle, E. R., & Perla, R. (1985). Field and laboratory measurements of snow liquid water by dilution. *Water Resources Research, 21*, 1415-1420. doi:10.1029/WR021i009p01415

Denoth, A. (1994). An electronic device for long-term snow wetness recording. *Annals of Glaciology, 19*, 104-106. doi:10.3189/S0260305500011058

Hefny, R., Kollar, L. E., Farzaneh, M., & Payrard, C. (2009). Adhesion of Wet Snow to Different Cable Surfaces. *Proc. 13th Int. Workshop on Atmospheric Icing of Structures.* Andermatt.

Incropera, F. P., & DeWitt, D. P. (1996). *Fundamentals of Heat and Mass Transfer* (4th ed.). New York: Wiley.

Jones, E. B., Rango, A., & Howell, S. M. (1983). Snowpack liquid water determinations using freezing calorimetry. *Hydrology Research, 14*, 113–126. doi:10.2166/nh.1983.0010

Kawashima, K., Endo, T., & Takeuchi, Y. (1998). A portable calorimeter for measuring liquid water content of wet snow. *Annals of Glaciology, 26*, 103-106. doi:10.3189/1998AoG26-1-103-106

Marcacci, P., Lacavalla, M., & Pirovano, G. (2019). Monitoring, measurements and mitigation for wet snow accretion on overhead conductors. *Proc. Int. Workshop on Atmospheric Icing of Structures.* Reykjavík, Iceland.

317 Sihvola, A., & Tiuri, M. (1986). Snow Fork for Field Determination of the Density and Wetness Profiles of a
318 Snow Pack. *IEEE Transactions on Geoscience and Remote Sensing, GE-24*, 717-721.
319 doi:10.1109/TGRS.1986.289619

320

321 APPENDIX A: STEEL CALORIMETER CONSTANT UNCERTAINTY

322 Considering the expression of E and r_{eq} in equations (5) and (12) respectively, the uncertainty associated to
323 the calorimeter constant and the equivalent ratio, are computed by making use of the well know propagation
324 error formula. Given the structure of the linear fit in equation A1, with $y = E$ and $x = r_{eq}$,

$$y = a_0 + a_1 x \tag{A1}$$

325 the expressions of the two adjustable regression parameters are:

$$a_0 = \langle y \rangle - a_1 \langle x \rangle \,,\; a_1 = \frac{\langle xy \rangle - \langle x \rangle \langle y \rangle}{\langle x^2 \rangle - \langle x \rangle^2} \tag{A2}$$

326 with

$$\begin{aligned} \langle x \rangle &= \frac{1}{n}\sum_{i=1}^{n} x_i & \langle y \rangle &= \frac{1}{n}\sum_{i=1}^{n} y_i \\ \langle xy \rangle &= \frac{1}{n}\sum_{i=1}^{n} x_i y_i & \langle x^2 \rangle &= \frac{1}{n}\sum_{i=1}^{n} x_i^2 \end{aligned} \tag{A3}$$

327 Once again, the uncertainty of the two parameters is computed according to the propagation formula as:

$$u_{a_0} = \sqrt{\sum_{i=1}^{n}\left(\frac{\partial a_0}{\partial x_i} u_{x_i}\right)^2 + \sum_{i=1}^{n}\left(\frac{\partial a_0}{\partial y_i} u_{y_i}\right)^2} \tag{A4}$$

$$u_{a_1} = \sqrt{\sum_{i=1}^{n}\left(\frac{\partial a_1}{\partial x_i} u_{x_i}\right)^2 + \sum_{i=1}^{n}\left(\frac{\partial a_1}{\partial y_i} u_{y_i}\right)^2} \tag{A5}$$

328 Being

$$\frac{\partial a_0}{\partial x_i} = -\frac{a_1}{n} - \frac{\partial a_1}{\partial x_i}\langle x \rangle \tag{A6a}$$

$$\frac{\partial a_0}{\partial y_i} = \frac{1}{n} + \frac{\partial a_1}{\partial y_i}\langle x \rangle \tag{A6b}$$

$$\frac{\partial a_1}{\partial x_i} = \frac{1}{n}\frac{(\langle x^2\rangle - \langle x\rangle^2)(y_i - \langle y\rangle) - 2(\langle xy\rangle - \langle x\rangle\langle y\rangle)(x_i - \langle x\rangle)}{(\langle x^2\rangle - \langle x\rangle^2)^2} \quad \text{(A6c)}$$

$$\frac{\partial a_1}{\partial y_i} = \frac{1}{n}\frac{x_i - \langle x\rangle}{\langle x^2\rangle - \langle x\rangle^2} \quad \text{(A6d)}$$

329 leading to the following expression for the regression line:

$$\hat{y}(x) = (29.3 \pm 3.3)x + (0.1 \pm 1.9) \quad \text{(A7)}$$

330 ($u_{a_1} = 3.3\ g$, $u_{a_0} = 1.9$ g).

331 It is worth noting that:

332 - the contribution of the uncertainty of equivalent ratio (the x variable) to the overall one is negligible.

333 - the intercept a_0 is also negligible, as it is an order of magnitude smaller than its own uncertainty and two

334 orders smaller than the x coefficient; therfore, it has been dropped in the final relation.

335 The uncertainty $u_{\hat{y}}$ associated with the predicted value is computed as:

$$u_{\hat{y}}(x_i) = \sqrt{\left(\frac{\partial \hat{y}}{\partial a_1}u_{a_1}\right)^2 + \left(\frac{\partial \hat{y}}{\partial a_0}u_{a_0}\right)^2} = \sqrt{x_i^2 u_{a_1}^2 + u_{a_0}^2} \quad \text{(A8)}$$

336 Which leads to the set of equation used to estimate the value and the uncertainty of the calorimeter constant

337 and reported in equation (13).